Coexistence of the antiferromagnetic and superconducting order and its effect on spin dynamics in electron-doped high-$T_c$ cuprates



2010 J. Phys.: Condens. Matter 22 035701

(http://iopscience.iop.org/0953-8984/22/3/035701)

J. Phys.: Condens. Matter **22** (2010) 035701 (7pp) doi:10.1088/0953-8984/22/3/035701

# Coexistence of the antiferromagnetic and superconducting order and its effect on spin dynamics in electron-doped high-$T_c$ cuprates

**Cui-Ping Chen, Hong-Min Jiang and Jian-Xin Li**

National Laboratory of Solid State Microstructures and Department of Physics, Nanjing University, Nanjing 210093, People's Republic of China

Received 22 October 2009
Published 16 December 2009
Online at stacks.iop.org/JPhysCM/22/035701

**Abstract**

In the framework of the slave-boson approach to the $t$–$t'$–$t''$–$J$ model, it is found that for electron-doped high-$T_c$ cuprates, the staggered antiferromagnetic (AF) order coexists with the superconducting (SC) order in a wide doping level ranged from underdoped to nearly optimally doped at the mean-field level. In the coexisting phase, it is revealed that the spin response is commensurate in a substantial frequency range below a crossover frequency $\omega_c$ for all dopings considered, and it switches to the incommensurate structure when the frequency is higher than $\omega_c$. This result is in agreement with the experimental measurements. Comparison of the spin response between the coexisting phase and the pure SC phase with a $d_{x^2-y^2}$-wave pairing plus a higher harmonics term (DP + HH) suggests that the inclusion of the two-band effect is important to consistently account for both the dispersion of the spin response and the non-monotonic gap behavior in the electron-doped cuprates.

(Some figures in this article are in colour only in the electronic version)

## 1. Introduction

The pairing symmetry of the hole-doped high-$T_c$ superconductors is generally believed to have the dominant $d_{x^2-y^2}$-wave pairing. However, the pairing symmetry of the electron-doped high-$T_c$ superconductors is still under debate [1–8]. While no consensus has been reached yet, more and more recent experimental results have suggested that the order parameter of electron-doped cuprates is likely to have a dominant $d_{x^2-y^2}$-wave pairing symmetry [3–8], and with an unusual non-monotonic gap function.

Although various explanations have been proposed to account for the non-monotonic behavior, they can generally be categorized into two scenarios [5, 7, 9–18]. One is to extend the superconducting (SC) gap out of the simplest $d_{x^2-y^2}$-wave via the inclusion of a higher harmonics term (DP + HH), i.e., the gap function can be written in the form $\Delta_k = \Delta_0[B(\cos k_x - \cos k_y) + (1 - B)(\cos 2k_x - \cos 2k_y)]$ [5, 7, 9–13]. From a theoretical perspective, the non-monotonic $d_{x^2-y^2}$-wave gap appears under the assumption that the $d_{x^2-y^2}$-wave pairing is caused by the interaction with the continuum of overdamped antiferromagnetic (AF) spin fluctuations. In this scenario, the non-monotonic gap behavior is described by the combination effect of a $d_{x^2-y^2}$-wave pairing plus a higher harmonics term. Therefore, it is an intrinsic property of the SC state regardless of the presence of the AF order, and a simple one-band model can reproduce the non-monotonic gap behavior. The other argues that the non-monotonic behavior is the outcome of the coexistence of the AF and the SC orders [14–18]. This scenario assumes that the AF order disguises the $d_{x^2-y^2}$-wave character of the SC gap. When the AF order is introduced, the resulting quasiparticle (QP) excitation can be gapped by both orders and behaves non-monotonically, although the SC gap itself is monotonic. The scenario gained support from angle-resolved photoemission spectra (ARPES) measurements, where two inequivalent Fermi pockets around $(\pi, 0)$ and $(\pi/2, \pi/2)$ have been detected [19, 20]. This phenomena is well explained in terms of the **k**-dependent band-folding effect associated with an AF order which splits the band into upper and lower branches [14, 20–22], leading to the two-band and/or two-gap model.

 

Recently, neutron scattering experiments in electron-doped cuprates have revealed that the spin response is commensurate in a substantial frequency range below a crossover frequency $\omega_c$ [23–28], which constitutes a distinct difference from the widely studied hourglass dispersion in hole-doped cuprates [29]. Although, both scenarios mentioned above can account for the non-monotonic gap behavior of the electron-doped cuprates, a comparative study on the spin dynamics between the two scenarios is needed to demonstrate the possible differences and therefore serve to select a reasonable model for electron-doped high-$T_c$ cuprates.

In this paper, we investigate the spin dynamics in the coexisting phase of the AF and the $d_{x^2-y^2}$-wave SC orders, and compare them with that in DP + HH. The calculation is based on a self-consistent determination of the QP dispersion, the AF order and the SC gap at the slave-boson mean-field level of the $t$–$t'$–$t''$–$J$ model. It is shown that the AF and SC orders compete and coexist in a substantial doping range in the underdoped regime. The spin response is commensurate below a crossover frequency $\omega_c$ for all dopings considered, and it becomes incommensurate when the frequency is higher than $\omega_c$. This result is qualitatively consistent with experiments [23–28]. While in the framework of the pure SC state with the $d_{x^2-y^2}$-wave and/or DP + HH [30–32], though an extended region of a commensurate spin fluctuation also exists, it evolves into an incommensurate spin fluctuation at low frequencies, which is not consistent with experiments. Therefore, our result suggests that the inclusion of the two-band effect resulting from the coexisting AF and SC orders is important to consistently account for both the spin dynamics and the non-monotonic gap behavior in the electron-doped cuprates.

The paper is organized as follows. In section 2, we introduce the theoretical model and carry out the analytical calculations. In section 3, we present the numerical results with some discussions. Finally, we present the conclusion in section 4.

## 2. Theoretical model

The Hamiltonian of the two dimensional $t$–$t'$–$t''$–$J$ model on a square lattice is written in the form,

$$\begin{aligned} H = &-t\sum_{\langle ij\rangle,\sigma}(c^\dagger_{i\sigma}c_{j\sigma}+\text{h.c.}) - t_1\sum_{\langle ij\rangle_2,\sigma}(c^\dagger_{i\sigma}c_{j\sigma}+\text{h.c.}) \\ &- t_2\sum_{\langle ij\rangle_3,\sigma}(c^\dagger_{i\sigma}c_{j\sigma}+\text{h.c.}) + J\sum_{\langle ij\rangle}(\mathbf{S}_i\cdot\mathbf{S}_j-\tfrac{1}{4}n_in_j) \\ &- \mu_0\sum_{\langle i\rangle,\sigma}c^\dagger_{i\sigma}c_{i\sigma}, \end{aligned} \tag{1}$$

where the summations $\langle ij\rangle$, $\langle ij\rangle_2$, $\langle ij\rangle_3$ run over the nearest-neighbor(n·n), the next-n·n, and the third-n·n pairs respectively, and $\mathbf{S}_i$ is the spin on site $i$. This Hamiltonian can be used to model both hole-doped and electron-doped systems after a particle–hole transformation. For electron-doping, one has $t < 0$, $t_1 > 0$ and $t_2 < 0$. The slave-boson mean-field theory is used to decouple the electron operators $c_{i\sigma}$ to bosons $b_i$ carrying the charge and fermions $f_{i\sigma}$ representing the spin. Then, the local constraint $b^\dagger_i b_i + \sum_\sigma f^\dagger_{i\sigma}f_{i\sigma} = 1$ is satisfied on average at the mean-field (MF) level. We choose the spinon pairing order $\Delta_{ij} = \langle f_{i\uparrow}f_{j\downarrow} - f_{i\downarrow}f_{j\uparrow}\rangle = \pm\Delta$, where $\Delta_{ij} = \Delta(-\Delta)$ for bond $\langle ij\rangle$ along the $x(y)$ direction, the uniform bond order $\chi_{ij} = \sum_\sigma\langle f^\dagger_{i\sigma}f_{j\sigma}\rangle = \chi$, the AF order $\langle f^\dagger_{i\uparrow}f_{i\uparrow} - f^\dagger_{i\downarrow}f_{i\downarrow}\rangle/2 = (-1)^i m$, and replace $b_i$ by $\langle b_i\rangle = \sqrt{x}$ due to boson condensation. After the Fourier transformation, the mean-field (MF) Hamiltonian can be written in the Nambu representation,

$$H = \sum_{\mathbf{k}} C^\dagger(\mathbf{k})\hat{A}(\mathbf{k})C(\mathbf{k}) + 2NJ(\chi^2+m^2+\Delta^2/2) - N\mu, \tag{2}$$

where the Nambu operator $C^\dagger(\mathbf{k}) = (f^\dagger_{\mathbf{k}\uparrow}, f^\dagger_{\mathbf{k}+\mathbf{Q}\uparrow}, f_{-\mathbf{k}\downarrow}, f_{-\mathbf{k}-\mathbf{Q}\downarrow})$ and

$$\hat{A}(\mathbf{k}) = \begin{pmatrix} \epsilon_{\mathbf{k}} & -2Jm & -J\Delta_{\mathbf{k}} & 0 \\ -2Jm & \epsilon_{\mathbf{k}+\mathbf{Q}} & 0 & J\Delta_{\mathbf{k}} \\ -J\Delta_{\mathbf{k}} & 0 & -\epsilon_{\mathbf{k}} & -2Jm \\ 0 & J\Delta_{\mathbf{k}} & -2Jm & -\epsilon_{\mathbf{k}+\mathbf{Q}} \end{pmatrix}, \tag{3}$$

where $\epsilon_{\mathbf{k}} = (-2tx - J\chi)(\cos k_x + \cos k_y) - 4t_1 x\cos k_x\cos k_y - 2t_2 x(\cos 2k_x + \cos 2k_y) - \mu$ and $\Delta_{\mathbf{k}} = \Delta(\cos k_x - \cos k_y)$. $\mu$ is the renormalized chemical potential, $N$ is the total number of lattice sites and $\mathbf{Q} = (\pi,\pi)$ is the AF momentum. Note that the wavevector $\mathbf{k}$ is restricted to the magnetic Brillouin zone (MBZ) in all that follows.

Diagonalizing the Hamiltonian (2) by a unitary matrix $\hat{U}(\mathbf{k})$ leads to four energy bands $E_1(\mathbf{k}) = E^+_{\mathbf{k}}$, $E_2(\mathbf{k}) = E^-_{\mathbf{k}}$, $E_3(\mathbf{k}) = -E^-_{\mathbf{k}}$, $E_4(\mathbf{k}) = -E^+_{\mathbf{k}}$, with

$$E^\pm_{\mathbf{k}} = \sqrt{(\xi^\pm_{\mathbf{k}})^2 + (J\Delta_{\mathbf{k}})^2}, \tag{4}$$

where $\xi^\pm_{\mathbf{k}} = \epsilon^+_{\mathbf{k}} \pm \sqrt{(\epsilon^-_{\mathbf{k}})^2 + 4J^2m^2}$ with $\epsilon^\pm_{\mathbf{k}} = (\epsilon_{\mathbf{k}} \pm \epsilon_{\mathbf{k}+\mathbf{Q}})/2$. Also, the free energy is written (Boltzmann constant $k_B = 1$) as

$$\begin{aligned} F = &-2T\sum_{\mathbf{k},\nu=\pm}\ln\left[2\cosh\left(\frac{E^\nu_{\mathbf{k}}}{2T}\right)\right] - \mu N \\ &+ 2NJ(\chi^2+m^2+\Delta^2/2). \end{aligned} \tag{5}$$

The MF order parameters $\chi$, $\Delta$, $m$ and the chemical potential $\mu$ for different dopings $x$ can be calculated from the self-consistent equations obtained by $\partial F/\partial\chi = 0$, $\partial F/\partial\Delta = 0$, $\partial F/\partial m = 0$, and $\partial F/\partial\mu = -N(1-x)$, respectively. The magnitudes of the parameters are chosen as $t = -3.0J$, $t_1 = 1.02J$, $t_2 = -0.51J$ and $J = 100$ meV [14]. Here we emphasize that the choice of parameters is conventional, and our results are not sensitive to the parameters.

Then, the bare spin susceptibility (transverse) is given by

$$\chi^\pm_0(\mathbf{q},\mathbf{q}',\tau) = \frac{1}{N}\langle S^+_{\mathbf{q}}(\tau)S^-_{-\mathbf{q}'}(0)\rangle_{(0)}, \tag{6}$$

where $\langle\cdots\rangle_{(0)}$ means thermal average over the eigenstates of $H$ and $S^+_{\mathbf{q}} = \sum_k f^+_{\mathbf{k}+\mathbf{q}\uparrow}f_{\mathbf{k}\downarrow}$ is the spin operator. Considering that $\mathbf{k}$ is restricted to the MBZ, an explicit calculation shows that the spin susceptibility should be expressed in the following matrix form:

$$\hat{\chi}^\pm_0(\mathbf{q},\omega) = \begin{pmatrix} \chi^\pm_0(\mathbf{q},\mathbf{q},\omega) & \chi^\pm_0(\mathbf{q},\mathbf{q}+\mathbf{Q},\omega) \\ \chi^\pm_0(\mathbf{q}+\mathbf{Q},\mathbf{q},\omega) & \chi^\pm_0(\mathbf{q}+\mathbf{Q},\mathbf{q}+\mathbf{Q},\omega) \end{pmatrix}, \tag{7}$$

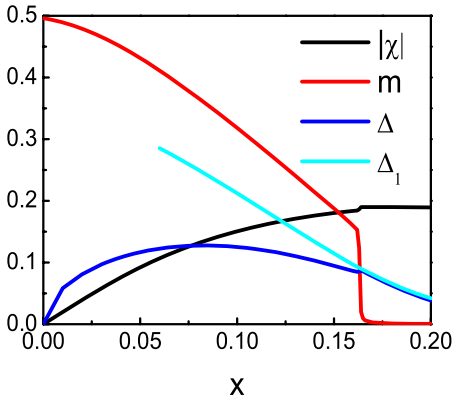


**Figure 1.** Mean-field phase diagram for the $t$–$t'$–$t''$–$J$ model, where $\Delta_1$ is the SC order parameter without considering the AF order. The model parameters are taken as $t = -3.0J$, $t' = 1.02J$ and $t'' = -0.51J$.

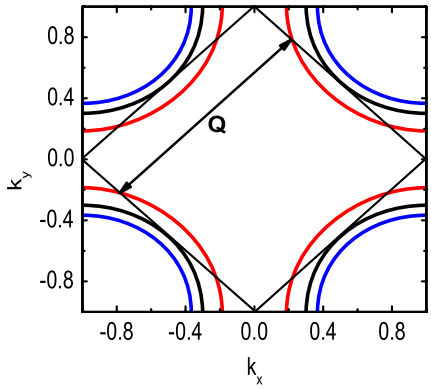


**Figure 2.** The Fermi surfaces without including the AF and SC orders. From outside to inside corresponds to doping concentration $x = 0.13, 0.165, 0.19$, respectively. The 'hot spots' on the Fermi surface are connected to each other by the vector **Q**.

where the nondiagonal correlation function $\chi_0^{\pm}$, with $\mathbf{q}' = \mathbf{q} + \mathbf{Q}$, arises due to the umklapp process. The matrix elements of the bare spin susceptibility, which come from the particle–hole ($p$–$h$) excitations, are given by,

$$\chi_0^{\pm}(\mathbf{q},\omega)_{\eta\eta'} = \frac{1}{N}\sum_{i,j=1}^{2}\sum_{m,n=1}^{2} \times \sum_{\mathbf{k}}\Bigg[a_1\frac{f(E_m(\mathbf{k})) - f(E_n(\mathbf{k}+\mathbf{q}))}{\omega + E_n(\mathbf{k}+\mathbf{q}) - E_m(\mathbf{k}) + \mathrm{i}\Gamma} + a_2\frac{f(E_n(\mathbf{k}+\mathbf{q})) - f(E_m(\mathbf{k}))}{\omega - E_n(\mathbf{k}+\mathbf{q}) + E_m(\mathbf{k}) + \mathrm{i}\Gamma} + b_1\frac{1 - f(E_m(\mathbf{k})) - f(E_n(\mathbf{k}+\mathbf{q}))}{\omega + E_n(\mathbf{k}+\mathbf{q}) + E_m(\mathbf{k}) + \mathrm{i}\Gamma} + b_2\frac{f(E_m(\mathbf{k})) + f(E_n(\mathbf{k}+\mathbf{q})) - 1}{\omega - E_n(\mathbf{k}+\mathbf{q}) - E_m(\mathbf{k}) + \mathrm{i}\Gamma}\Bigg], \tag{8}$$

where $f(E_{\mathbf{k}})$ is the Fermi function and

$$\begin{aligned} a_1 &= U^*_{in}(\mathbf{k}+\mathbf{q})U_{(j+\eta'-\eta)n}(\mathbf{k}+\mathbf{q})U_{im}(\mathbf{k})U^*_{jm}(\mathbf{k}) \\ &\quad + U^*_{in}(\mathbf{k}+\mathbf{q})U_{(j+2)n}(\mathbf{k}+\mathbf{q})U_{im}(\mathbf{k})U^*_{(j+2+\eta'-\eta)m}(\mathbf{k}), \\ a_2 &= U_{(i+2)n}(\mathbf{k}+\mathbf{q})U^*_{(j+2+\eta'-\eta)n}(\mathbf{k}+\mathbf{q})U^*_{(i+2)m}(k)U_{(j+2)m}(\mathbf{k}) \\ &\quad + U_{(i+2)n}(\mathbf{k}+\mathbf{q})U^*_{jn}(\mathbf{k}+\mathbf{q})U^*_{(i+2)m}(\mathbf{k})U_{(j+\eta'-\eta)m}(\mathbf{k}), \\ b_1 &= U^*_{in}(\mathbf{k}+\mathbf{q})U_{(j+\eta'-\eta)n}(\mathbf{k}+\mathbf{q})U^*_{(i+2)m}(\mathbf{k})U_{(j+2)m}(\mathbf{k}) \\ &\quad - U^*_{in}(\mathbf{k}+\mathbf{q})U_{(j+2)n}(\mathbf{k}+\mathbf{q})U^*_{(i+2)m}(\mathbf{k})U_{(j+\eta'-\eta)m}(\mathbf{k}), \\ b_2 &= U_{(i+2)n}(\mathbf{k}+\mathbf{q})U^*_{(j+2+\eta'-\eta)n}(\mathbf{k}+\mathbf{q})U_{im}(\mathbf{k})U^*_{jm}(\mathbf{k}) \\ &\quad - U_{(i+2)n}(\mathbf{k}+\mathbf{q})U^*_{jn}(\mathbf{k}+\mathbf{q})U_{im}(\mathbf{k})U^*_{(j+2+\eta'-\eta)m}(\mathbf{k}). \end{aligned} \tag{9}$$

As for DP + HH, the model and calculation of the spin susceptibility are the same as [31].

The renormalized spin susceptibility due to the spin fluctuations is obtained via the random-phase approximation (RPA),

$$\hat{\chi}^{\pm}(\mathbf{q},\omega) = \frac{\hat{\chi}_0^{\pm}(\mathbf{q},\omega)}{\hat{1} + \alpha\hat{J}_q\hat{\chi}_0^{\pm}(\mathbf{q},\omega)}, \tag{10}$$

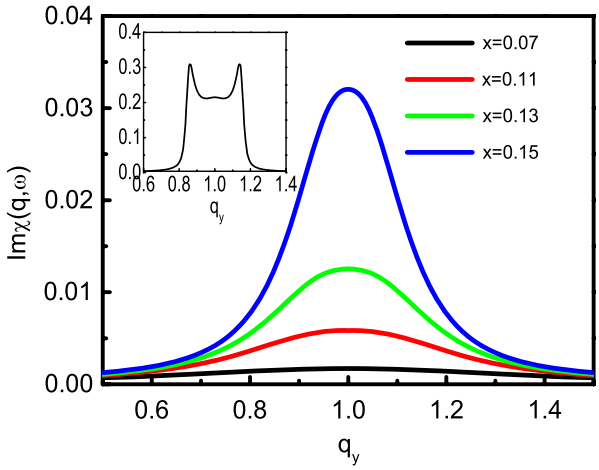


**Figure 3.** Doping dependence of Im $\chi(\mathbf{q}, \omega)$ in the coexisting phase of the AF and SC orders at low frequency $\omega = 0.04J$. The momentum is scanned along $(\pi, q_y)$. The inset shows Im $\chi(q, \omega)$ at $\omega = 0.04J$ for DP + HH [$\Delta_k = \Delta_0[(\cos k_x - \cos k_y) + B(\cos 2k_x - \cos 2k_y)]$] [31] at doping $x = 0.15$.

where

$$\hat{J}_q = \begin{pmatrix} J(\mathbf{q}) & 0 \\ 0 & J(\mathbf{q}+\mathbf{Q}) \end{pmatrix} \tag{11}$$

with $J(\mathbf{q}) = J(\cos q_x + \cos q_y)$. In the coexisting phase of the AF and SC orders, $\alpha$ is taken as 1. As for DP + HH, we choose a slightly small $\alpha = 0.634$. It is well known that the usual RPA with $\alpha = 1$ overestimates the AF spin fluctuations. The criteria for choosing $\alpha$ is to set the AF instability at $x = 0.12$, which is the experimental observed value for $Nd_{2-x}Ce_xCuO_4$ (NCCO) [33]. The parameter $\Gamma = 0.04J$ is introduced to account of the QP damping rate, which comes from the scattering off other fluctuations that are not included here.

## 3. Numerical results and discussion

In figure 1, we show the MF parameters $\chi$, $m$ and $\Delta$ as a function of doping $x$. For a comparison, we also show the doping dependence of the MF SC gap $\Delta_1$, obtained without

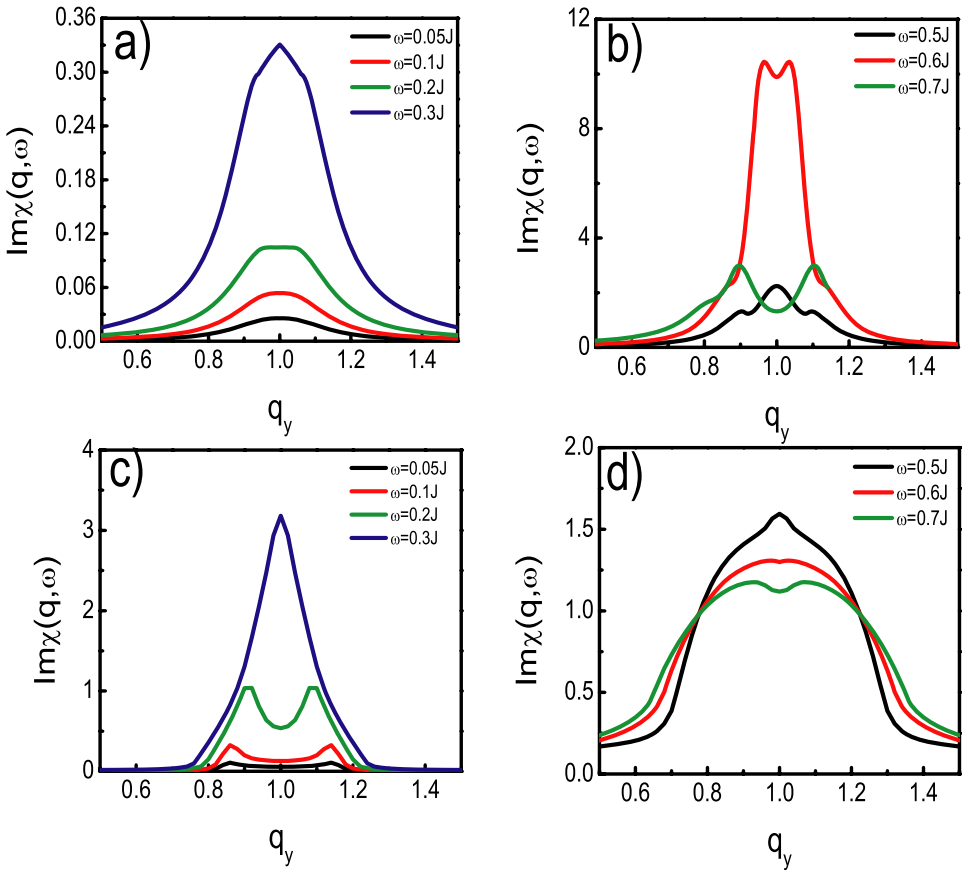


**Figure 4.** Frequency dependence of Im $\chi(\mathbf{q}, \omega)$ at doping $x = 0.15$. The momentum is scanned along $(\pi, q_y)$. (a) and (b) are in the coexistence of the AF and SC states. (c) and (d) are in DP + HH [$\Delta_k = \Delta[(\cos k_x - \cos k_y) + B(\cos 2k_x - \cos 2k_y)]$] [31].

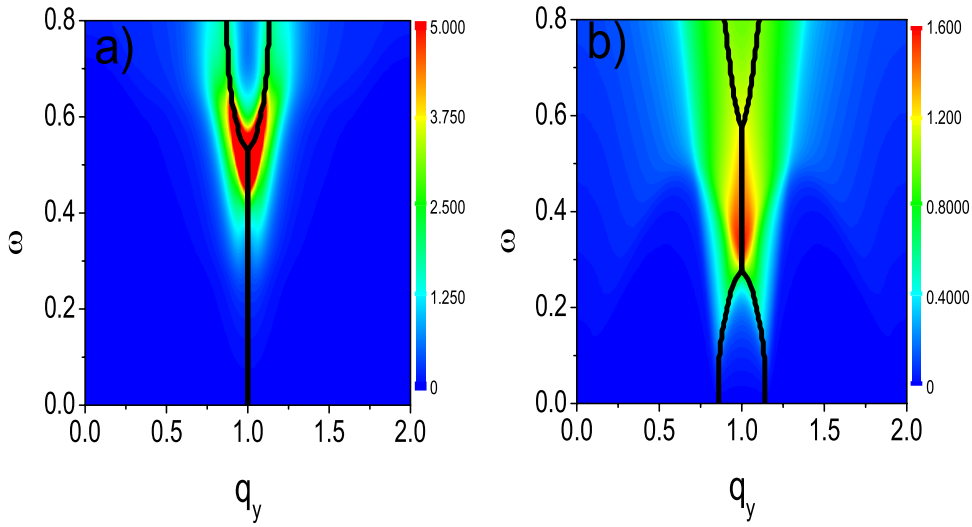


**Figure 5.** Intensity plot of Im $\chi(\mathbf{q}, \omega)$ as a function of frequency ($\omega$) and momentum ($\mathbf{q}$) at doping $x = 0.15$. The momentum is scanned along $(\pi, q_y)$. The solid line is the peak position. (a) is in the coexistence of the AF and SC states and (b) in DP + HH [$\Delta_k = \Delta[(\cos k_x - \cos k_y) + B(\cos 2k_x - \cos 2k_y)]$] [31].

considering the AF order by setting $m = 0$. It is seen that the staggered magnetization $m$ decreases with increasing doping $x$, and goes sharply to zero at $x \approx 0.165$, which implies a phase transition from the antiferromagnetic (AFM) phase to the paramagnetic phase. The SC order parameter, on the other hand, initially increases in value up to an optimal doping level, and then decreases upon further doping, forming a generic SC dome [34]. However, the SC order parameter $\Delta_1$, without the inclusion of the AF order, exhibits a monotonic decrease with doping, which obviously deviates from the experimental

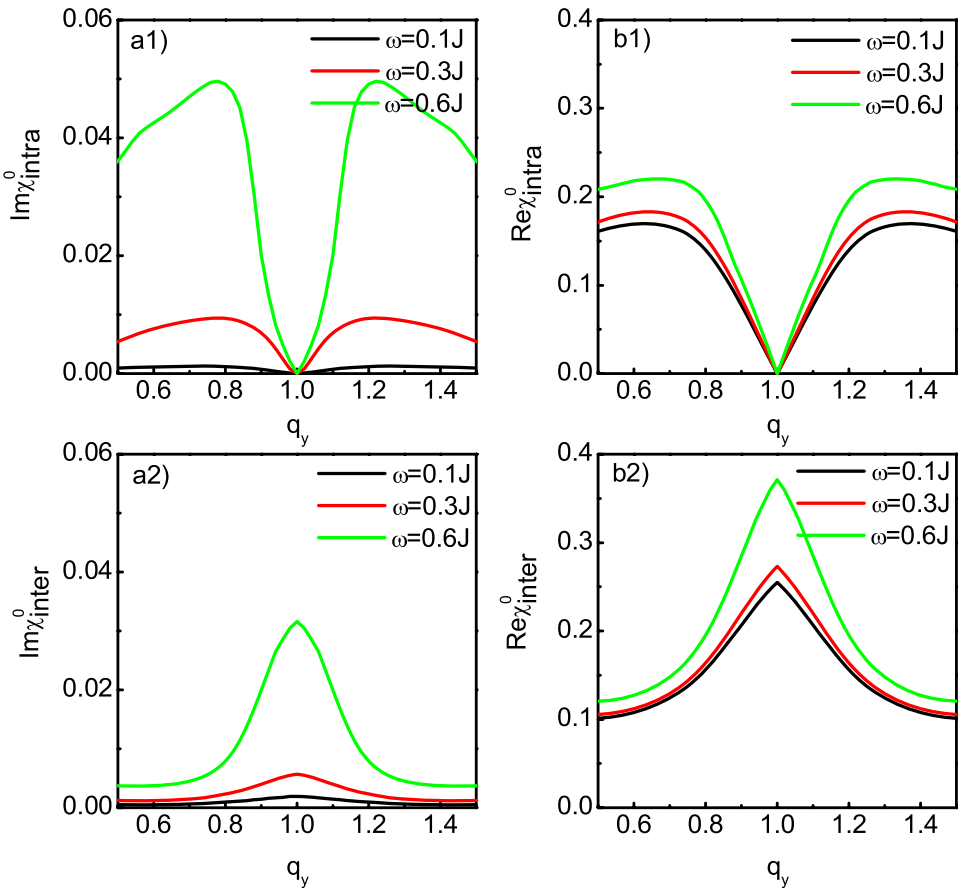


**Figure 6.** Frequency dependence of the intra- and inter-band contributions to the bare spin susceptibility $\chi_0(\mathbf{q}, \omega)$ ((a1) and (a2) denote the imaginary part, (b1) and (b2) the real part) in the coexistence of AF and SC states at doping $x = 0.15$. (a1) and (b1) show the intra-band contributions, and (a2) and (b2) the inter-band contribution.

observations. Furthermore, the SC order parameter $\Delta$ with an AF order shows a noticeable suppression compared to $\Delta_1$, and exhibits a competitive character with the AF order. However, they also coexist in a substantial doping range.

It should be pointed out that figure 1 is just the slave-boson mean-field phase diagram, the survival of the SC order at very low doping does not mean the existence of a SC phase in the actual system with the same doping. This is due to the fact that the slave-boson approach to the $t$–$J$ model works well in the metallic state of the cuprates after doping, and fails in the very low doping regime where the insulating AF order is found in the experiments. However, the similarity of the phase diagram obtained by the slave-boson mean-field theory to that of the variational quantum-cluster theory [16, 22] validates the SBMFT as a low energy effective theory. Also, a similar phase diagram has been obtained before [15].

We note that, at the critical doping $x \approx 0.165$, the AF order parameter $m$ jumps to almost $1/3$ of its maximum value whereas the SC order $\Delta$ is less affected. This feature may be understood by the evolution of the Fermi surface with doping, as shown in figure 2. We can see that with the increase of electron-doping, the Fermi surface shrinks and moves towards the $M = (\pi, \pi)$ point. As a result, the 'hot spots' (the cross points between the Fermi surface and the boundary of the MBZ) move towards the Brillouin zone diagonals, and eventually disappear at doping $x \approx 0.165$. On the other hand, the AF order has an order wavevector $(\pi, \pi)$, which is related to the particle–hole excitations from one 'hot spot' to another. Accordingly, the existence of the 'hot spots' is necessary for the formation of the AFM order, while there is no such requirement for the SC order. Therefore, the disappearance of the 'hot spots' leads to a vanishing AF order, but has less effect on the SC order.

The doping dependence of the renormalized spin susceptibility $\mathrm{Im}\,\chi(\mathbf{q}, \omega)$ at a low frequency $\omega = 0.04J$ in the coexisting phase is presented in figure 3. In this figure, it is found that the low energy excitations exhibit commensurate peaks for all $x$, which is very consistent with the experiments [27]. The inset shows the spin susceptibility $\mathrm{Im}\,\chi(\mathbf{q}, \omega)$ at doping $x = 0.15$ in DP + HH. One can see that the spin response is incommensurate at low frequency without considering the AF order.

Detailed frequency dependence of the spin response in the coexisting phase and DP + HH at doping $x = 0.15$ are shown in figures 4(a) and (b), and figures 4(c) and (d), respectively. The difference in the low frequency regime of the two phases is more evident here. The spin fluctuation is commensurate in a substantial frequency range below a crossover frequency $\omega_c \approx 0.52J$ and down to the lowest frequency considered in the coexisting phase, and switches to

be incommensurate when the frequency is higher than $\omega_c \approx 0.52J$ (figure 5(a)). This feature agrees with the neutron scattering measurements on electron-doped cuprates that have been reported recently [23]. Whereas for DP + HH, the spin response is incommensurate at low frequency, then switches to be commensurate within the intermediate frequency range, and becomes incommensurate again at higher frequency [31]. These results can be summarized in the intensity plot of the imaginary part of the renormalized spin susceptibility $\mathrm{Im}\,\chi(\mathbf{q},\omega)$ as a function of frequency and momentum along the $(\pi, q_y)$ direction, shown in figure 5. In the figure, the solid line indicating the peak position is the dispersion of spin excitations. The commensurate spin fluctuation prevails below $\omega_c$ for the coexisting system (figure 5(a)). For DP + HH, the dispersion shows an hourglass-like behavior (figure 5(b)), which is similar to the hole-doped one, and is not consistent with the experiments on electron-doped cuprates [23].

In the presence of the AF order, the energy band of QP is split into two bands. Therefore, the particle–hole excitations that contributed to the spin susceptibility are composed of two kinds of excitations, the intra-band and the inter-band excitations. In figure 6, we present the results for the bare spin susceptibility $\chi_0(\mathbf{q},\omega)$ (without the RPA correction) coming from the intra-band and the inter-band contributions, respectively. Figures 6(a1) and (a2) denote the imaginary part of $\chi_0(\mathbf{q},\omega)$, figures 6(b1) and (b2) the real part. One obvious feature is that, the intra-band contribution is zero at the AF momentum $\mathbf{Q}$, leading to the incommensurate spin response. It results from the fact that the coherence factor in the spin susceptibility due to the intra-band excitations, $1 - [(2Jm)^2 - \varepsilon_{\mathbf{k}+\mathbf{q}}\varepsilon_{\mathbf{k}}]/[\sqrt{\varepsilon^2_{\mathbf{k}+\mathbf{q}} + (2Jm)^2}\sqrt{\varepsilon^2_{\mathbf{k}} + (2Jm)^2}]$ (where, $\varepsilon_{\mathbf{k}} = (-2tx - J\chi)(\cos k_x + \cos k_y)$) is zero at $\mathbf{Q}$. Whereas, the inter-band contribution is commensurate for all frequencies. At low frequencies, the inter-band excitations have a larger contribution to the spin susceptibility than the intra-band excitations, so the spin fluctuation is commensurate. However, with an increase of frequency, the intensity of $\mathrm{Im}\,\chi_0(\mathbf{q},\omega)$ due to the intra-band contributions increases more rapidly than the inter-band contribution. As a result, the spin fluctuation switches from a commensurate to an incommensurate structure.

## 4. Conclusion

In this paper, we have investigated the spin dynamics in electron-doped cuprates in the coexisting phase of the $d_{x^2-y^2}$-wave SC and AF orders, and compared the results with that in DP + HH. Both coexisting phase and DP + HH can account for the non-monotonic gap behavior of the electron-doped cuprates (that is, the maximum of $\Delta_k$ along the Fermi surface is located at the 'hot spots'), but their spin response is different.

In the coexisting phase, we found that the spin response is commensurate in a substantial frequency range below a crossover frequency $\omega_c$ for all dopings considered, and it switches to be incommensurate when the frequency is higher than $\omega_c$. The theoretical calculations are shown to be in good agreement with the experimental measurements. However, in DP + HH, the spin response is incommensurate at low frequency, and the dispersion is just like that of the hole-doped one, namely exhibits an hourglass-like dispersion.

Thus, our result suggests that the inclusion of the two-band effect is important to consistently account for both the dispersion of the spin response and the non-monotonic gap behavior in the electron-doped cuprates.

## Acknowledgments

This work was supported by the National Natural Science Foundation of China (10525415, 10904062) and the Ministry of Science and Technology of China (973 project Grants Nos 2006CB601002, 2006CB921800).

## References

[1] Tsuei C C and Kirtley J R 2000 *Phys. Rev. Lett.* **85** 182
Darminto A D, Smilde H J H, Leca V, Blank D H A, Rogalla H and Hilgenkamp H 2005 *Phys. Rev. Lett.* **94** 167001
Biswas A, Fournier P, Qazilbash M M, Smolyaninova V N, Balci H and Greene R L 2002 *Phys. Rev. Lett.* **88** 207004
[2] Shan L, Huang Y, Wang Y L, Li S, Zhao J, Dai P, Zhang Y Z, Ren C and Wen H H 2008 *Phys. Rev.* B **77** 014526
Zimmers A, Noat Y, Cren T, Sacks W, Roditchev D, Liang B and Greene R L 2007 *Phys. Rev.* B **76** 132505
Zheng G-Q, Sato T, Kitaoka Y, Fujita M and Yamada K 2003 *Phys. Rev. Lett.* **90** 197005
Skinta J A, Kim M-S, Lemberger T R, Greibe T and Naito M 2002 *Phys. Rev. Lett.* **88** 207005
[3] Sato T, Kamiyama T, Takahashi T, Kurahashi K and Yamada K 2001 *Science* **291** 1517
[4] Armitage N P, Lu D H, Feng D L, Kim C, Damascelli A, Shen K M, Ronning F, Shen Z X, Onose Y, Taguchi Y and Tokura Y 2001 *Phys. Rev. Lett.* **86** 1126
[5] Matsui H, Terashima K, Sato T, Takahashi T, Fujita M and Yamada K 2005 *Phys. Rev. Lett.* **95** 017003
[6] Park S R, Roh Y S, Yoon Y K, Leem C S, Kim J H, Kim B J, Koh H, Eisaki H, Armitage N P and Kim C 2007 *Phys. Rev.* B **75** 060501(R)
[7] Blumberg G, Koitzsch A, Gozar A, Dennis B S, Kendziora C A, Fournier P and Greene R L 2002 *Phys. Rev. Lett.* **88** 107002
[8] Dagan Y, Beck R and Greene R L 2007 *Phys. Rev. Lett.* **99** 147004
[9] Krotkov P and Chubukov A V 2006 *Phys. Rev. Lett.* **96** 107002
[10] Yoshimura H and Hirashima D S 2005 *J. Phys. Soc. Japan* **73** 2057
Yoshimura H and Hirashima D S 2005 *J. Phys. Soc. Japan* **74** 712
[11] Khodel V A, Yakovenko V M, Zverev M V and Kang H 2004 *Phys. Rev.* B **69** 144501
[12] Watanabe T, Miyata T, Yokoyama H, Tanaka Y and Inoue J-I 2005 *J. Phys. Soc. Japan* **74** 1942
[13] Krotkov P and Chubukov A V 2006 *Phys. Rev.* B **74** 014509
[14] Yuan Q S, Yuan F and Ting C S 2006 *Phys. Rev.* B **73** 054501
Yuan Q S, Yan X Z and Ting C S 2006 *Phys. Rev.* B **74** 214503
[15] Yuan W, Lü H-D, Lu H-Y and Wang Q-H 2008 *Phys. Rev.* B **77** 064515
[16] Das T, Markiewicz R S and Bansil A 2006 *Phys. Rev.* B **74** 020506(R)
Aichhorn M, Arrigoni E, Potthoff M and Hanke W 2006 *Phys. Rev.* B **74** 024508
[17] Luo H G and Xiang T 2005 *Phys. Rev. Lett.* **94** 027001
[18] Liu C S, Luo H G, Wu W C and Xiang T 2006 *Phys. Rev.* B **73** 174517

[19] Armitage N P, Ronning F, Lu D H, Kim C, Damascelli A, Shen K M, Feng D L, Eisaki H, Shen Z-X, Mang P K, Kaneko N, Greven M, Onose Y, Taguchi Y and Tokura Y 2002 *Phys. Rev. Lett.* **88** 257001
[20] Matsui H, Terashima K, Sato T, Takahashi T, Wang S-C, Yang H-B, Ding H, Uefuji T and Yamada K 2005 *Phys. Rev. Lett.* **94** 047005
[21] Kusko C, Markiewicz R S, Lindroos M and Bansil A 2002 *Phys. Rev.* B **66** 140513(R)
[22] Sénéchal D, Lavertu P-L, Marois M-A and Tremblay A-M S 2005 *Phys. Rev. Lett.* **94** 156404
[23] Wilson S D, Li S, Woo H, Dai P, Mook H A, Frost C D, Komiya S and Ando Y 2006 *Phys. Rev. Lett.* **96** 157001
[24] Yamada K, Kurahashi K, Uefuji T, Park S, Lee S-H and Endoh Y 2003 *Phys. Rev. Lett.* **90** 137004
[25] Kang H J, Dai P, Mook H A, Argyriou D N, Sikolenko V, Lynn J W, Kurita Y, Komiya S and Ando Y 2005 *Phys. Rev.* B **71** 214512
[26] Wilson S D, Li S, Dai P, Bao W, Chung J, Kang H J, Lee S H, Komiya S, Ando Y and Si Q 2006 *Phys. Rev.* B **74** 144514
[27] Fujita M, Matsuda M, Lee S-H, Nakagawa M and Yamada K 2008 *Phys. Rev. Lett.* **101** 107003
[28] Motoyama E M, Yu G, Vishik I M, Vajk O P, Mang P K and Greven M 2007 *Nature* **445** 186
[29] Bourges P, Sidis Y, Fong H F, Renault L P, Bossy J, Ivanov A and Keimer B 2000 *Science* **288** 1234
Dai P, Mook A, Hunt R D and Dogan F 2001 *Phys. Rev.* B **63** 054525
Hayden S M, Mook H A, Dai P, Perring T G and Dogan F 2004 *Nature* **429** 531
Tranquada J M, Woo H, Perring T G, Goka H, Gu G D, Xu G, Fujita M and Yamada K 2004 *Nature* **429** 534
[30] Li J X, Zhang J and Luo J 2003 *Phys. Rev.* B **68** 224503
[31] Chen C P, Zhou T and Li J X 2009 *Physica* C **469** 234
[32] Krüger K, Wilson S D, Shan L, Li S, Huang Y, Wen H-H, Zhang S-C, Dai P and Zaanen J 2007 *Phys. Rev.* B **76** 094506
[33] See e.g., Dagotto E 1994 *Rev. Mod. Phys.* **66** 763
[34] Lee P A, Nagaosa N and Wen X-G 2006 *Rev. Mod. Phys.* **78** 000017